NANO LETTERS

Letter

pubs.acs.org/NanoLett

Highly Efficient Perovskite Solar Cells with Tunable Structural Color

Wei Zhang,[†,§] Miguel Anaya,[‡,§] Gabriel Lozano,[‡] Mauricio E. Calvo,[‡] Michael B. Johnston,[†] Hernán Míguez,*[,‡] and Henry J. Snaith*[,†]

[†]Department of Physics, University of Oxford, Clarendon Laboratory, Parks Road, Oxford OX1 3PU, United Kingdom

[‡]Instituto de Ciencia de Materiales de Sevilla, Consejo Superior de Investigaciones, Científicas-Universidad de Sevilla, Calle Américo Vespucio 49, 41092 Sevilla, Spain

Supporting Information

ABSTRACT: The performance of perovskite solar cells has been progressing over the past few years and efficiency is likely to continue to increase. However, a negative aspect for the integration of perovskite solar cells in the built environment is that the color gamut available in these materials is very limited and does not cover the green-to-blue region of the visible spectrum, which has been a big selling point for organic photovoltaics. Here, we integrate a porous photonic crystal (PC) scaffold within the photoactive layer of an opaque perovskite solar cell following a bottom-up approach employing inexpensive and scalable liquid processing techniques. The photovoltaic devices presented herein show high efficiency with tunable color across the visible spectrum. This now imbues the perovskite solar cells with highly desirable properties for cladding in the built environment and encourages design of sustainable colorful buildings and iridescent electric vehicles as future power generation sources.

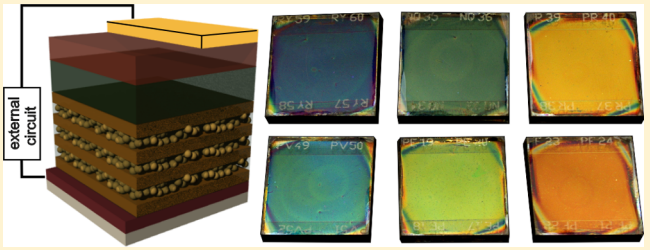

KEYWORDS: *Structural color, perovskite solar cells, building integrated photovoltaic, porous photonic crystal, multilayers*

Photovoltaic (PV) solar energy has the prospect to supply our global energy demands hundreds of times over. A large fraction of the cost of solar energy is not the solar cells but the fixed cost of land, frames, supports and services. A smart move to slash these fixed costs is to build the PV directly into the infrastructure and supports already constructed for other purposes, such as building facades, fences, walls, awnings, and automotive skins. However, for widespread uptake of building integrated PV (BIPV),[1] the PV has to be aesthetically versatile. Organic–inorganic halide perovskite solar cells have undergone rapid progress,[2−11] with efficiencies approaching those of existing thin film and silicon.[9] Perovskite solar cells are constructed by forming a polycrystalline layer of an organic–inorganic halide perovskite, typically $CH_3NH_3PbI_3$ or the mixed halide variant $CH_3NH_3PbI_{3-x}Cl_x$, sandwiched between an n-type and p-type charge collection layer.[6] In addition to this simple planar structure, the perovskite layer can be infiltrated into a mesoporous layer of n-type TiO_2 or insulating dielectric scaffolds.[3,4,7,12,13] Although significant advance has been made to achieve highly efficient perovskite solar cells, the negative aspect for perovskites in BIPV is that the color pallet available in these materials is very basic and, notably absent of greens and blues,[14,15] highly desirable in the built environment.

There has been significant previous work developing semitransparent solar cells, which is another key feature to consider for window applications in BIPV. In this regard, thinner perovskite layers have been already demonstrated to achieve semitransparent cells with high power conversion efficiencies.[16−18] However, strong coloration, and specifically blues and greens, has not been achieved. A solution may be to follow the route often employed by nature: structural colors, in contrast to pigments or dyes, arise from the interference of coherently scattered light waves. With the aim of endowing this type of device with color, we propose a versatile approach based on photonics rather than on chemical management because the latter has demonstrated limited success in the blue-to-green region of the spectrum.[14,15] Although the multilayer approach has been proven to be compatible with semitransparent devices,[19,20] in this study, we will focus on opaque cells and develop a multilayered scaffold that exhibits photonic crystal (PC) properties, which simultaneously provides optical reflection at selected visible wavelength ranges and allows good electrical contact with the charge collecting layers. We successfully achieve a broad gamut of iridescent solar cells, which deliver up to 8.8% efficiency with a blue hue.

The thickness of such a supporting porous structure is restricted by the charge transport properties of the perovskite, which typically imposes the scaffold to be no thicker than 400 nm in order to attain highly efficient devices, which are consequently nontransparent.[21] In order to integrate a photonic structure within a perovskite device, our initial attempts involved the substitution of the porous scaffold by a PC

Received: November 13, 2014
Revised: January 31, 2015
Published: February 4, 2015

DOI: 10.1021/nl504349z
Nano Lett. 2015, 15, 1698−1702

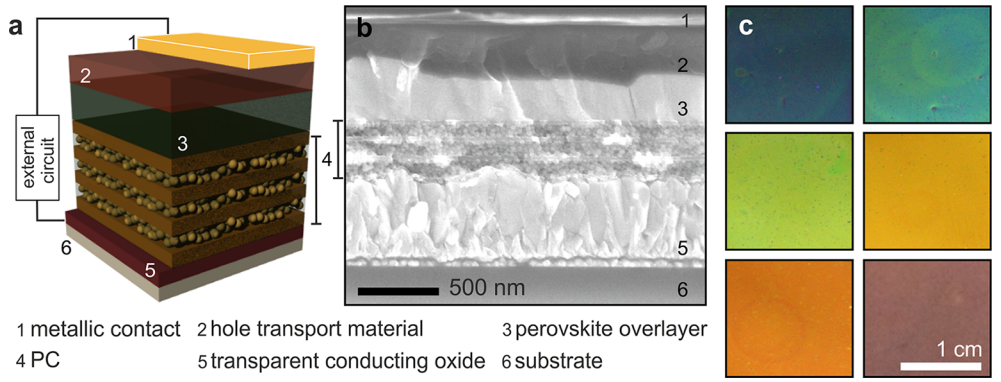

Figure 1. Structural and aesthetic characterization. (a) Scheme of a photonic-crystal (PC)-based perovskite solar cell. (b) Secondary electron scanning electron microscope image of a cross section of a PC-based solar cell. The PC is made by the alternated deposition of SiO_2 nanoparticles and TiO_2 layers. Devices under investigation are comprised of gold as metallic contact, spiro-OMeTAD as hole transport material, the PC is infiltrated by $CH_3NH_3PbI_{3-x}Cl_x$, and fluorinated tin oxide as transparent conducting oxide. The cell is deposited over a glass substrate. (c) Colors (from blue to red) displayed by devices integrating different PCs.

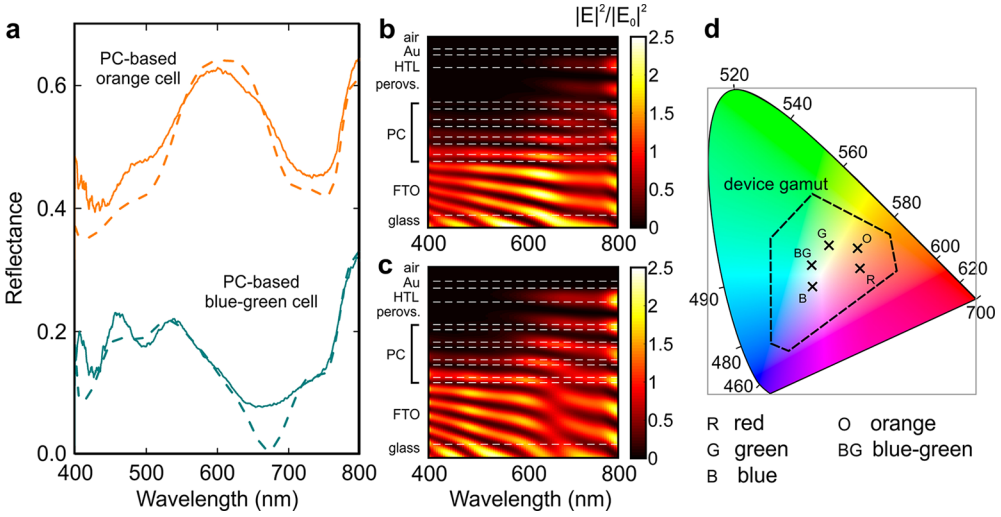

Figure 2. Color analysis. (a) Experimental (solid lines) and theoretical reflectance (dashed lines) of the PC-based orange (orange lines) and blue-green (dark cyan lines) perovskite solar cells. Orange curves are vertically shifted by $\Delta R = 0.3$ for the sake of clarity. (b–c) Calculated spatial (vertical axis) and spectral (horizontal axis) distribution of the square of the electric field enhancement ($|E|^2/|E_0|^2$), that is, the square of the electric field normalized by the square of the electric field in the incoming medium, along a cross section of the solar cell, for the PC-based (b) orange and (c) blue-green cells. Calculations were carried out considering the multilayer parameters extracted from the fittings of the reflectance measurements: (b) $d_H = 58$ nm, $d_L = 87$ nm and (c), $d_H = 39$ nm, $d_L = 90$ nm. Horizontal dashed lines are guides to the eye to delimit the interfaces between layers in the solar cells. The bottom of the images is the glass side, and the top, the gold electrode side. (d) CIE 1931 chromaticity space, showing the color hues of the PC-based (R) red (0.41, 0.34), (O) orange (0.41, 0.40), (G) green (0.33, 0.41), (BG) blue-green (0.29, 0.35), and (B) blue (0.29, 0.30) cells. The dashed black line delimits the device color gamut. It encompasses all different hues that can be achieved tuning the lattice parameter from 20 to 300 nm, and the thickness ratio of the high and low index material of the PC. The porosities of the high and low index materials, prior to perovskite infiltration, are considered to be 4% and 50%, respectively.

made by stacking nanoparticle layers of different kind,[22] following a recipe that had permitted the successful integration of colored mirrors in dye sensitized solar cells.[20] However, although we achieved efficient perovskite solar cells by this approach, the color they displayed was not different to that of nonstructured ones, since the refractive index contrast of the porous photonic crystal after perovskite infiltration was largely diminished. A potential solution to this problem is to increase the number of layers, so the reflections arising from the photonic crystal mirrors are stronger and color can be preserved after infiltration. Unfortunately, we found that such an approach rendered the device performance very poor, as we show in Supporting Information Figure S1, because the total scaffold thickness is double that of the optimum one. Thus, a balance between minimization of the photonic skeleton thickness and preservation of its high reflectance after infiltration is required. To meet this compromise, we devise multilayers in which the refractive index contrast between layers in the PC is maximized by grossly varying the porosity of each layer. In this way, the number of unit cells, and therefore the thickness, required to achieve a strong reflection peak can be reduced below the optimum scaffold size, but the perovskite precursors is still capable of soaking the photonic matrix. We employ layers of materials in different aggregation states that permitted us to tune the open porosity of each alternate layer. We make low and high refractive index layers by spin-coating SiO_2 nanoparticles and TiO_2 sol-gel precursors,[23] respectively, onto a fluorinated tin oxide (FTO) coated glass substrate. During the deposition of the multilayer "mirror", and in order to prevent infiltration of the TiO_2 precursors into the porous

DOI: 10.1021/nl504349z
Nano Lett. 2015, 15, 1698–1702

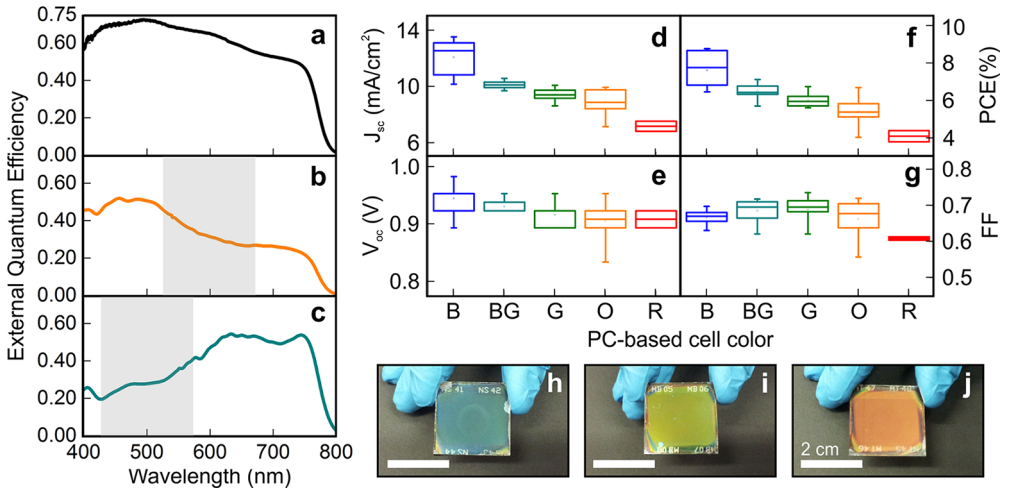

Figure 3. Electrical characterization and device performance analysis. (a–c) Spectral dependence of the external quantum efficiency of (a) a nonphotonic structured SiO_2 scaffold-based perovskite solar cell, which acts as a reference, (b) an *orange* PC-based cell, and (c) *blue-green* PC-based cell. The shaded areas correspond to the spectral regions in which the PC-based cells show high reflectance. (d–g) Box-plot of the device performance indicators for the different PC-based cells: (d) short-circuit current density (J_{sc}), (e) open circuit voltage (V_{oc}), (f) power conversion efficiency (PCE), and (g) fill factor (FF). (h–j) Digital camera pictures of the devices labeled as (h) blue, (i) green, and (j) orange.

SiO_2 layer, the latter is filled with a polymer. In this way, we form relatively dense (4% open porosity) layers of TiO_2 alternately onto hybrid polymer-SiO_2 layers. Subsequent sintering decomposes the polymer matrix and renders the SiO_2 layer porous again (50% open porosity). We obtained porosity and refractive index values (n_L = 1.25 and n_H = 2.38, at λ = 500 nm) from the optical analysis of the PCs. After depositing the perovskite precursors and annealing, we observe a strong red-shift of the reflectance peak of the multilayer (see Supporting Information Figure S2), which indicates that the mirror is being infiltrated by the perovskite semiconductor, resulting in a shift in the effective refractive index. In fact, from the fitting of the optical properties, we estimate that the perovskite completely fills the voids in both SiO_2 and TiO_2 layers, demonstrating their accessibility and interconnectivity, despite the very low porosity in the dense TiO_2 layers.

We show a schematic of the structure of the perovskite solar cell incorporating a three-unit-cell one-dimensional PC in Figure 1a and a scanning electron microscopy (SEM) image of a cross section of such a device in Figure 1b. This image reveals that the first SiO_2 nanoparticle layer is capable of leveling the roughness, characteristic of the FTO coating, thus providing a flat surface for subsequent layer deposition. Furthermore, back scattered electron image analysis shows that the infiltrated perovskite percolates through the void network of the photonic structure, which can then act as an electronic bridging path between the solid perovskite overlayer and the FTO anode. A study of the characteristics of the perovskite infiltration is provided as Supporting Information (see Figure S2). As we show in the photographs of constructed solar cells in Figure 1c, the obtained devices show intense colors variable across the visible spectrum. We can precisely tune the reflectance peak of the PC by modifying the thickness of the individual layers. The vivid iridescences observed are achieved by the combination of reflection from the PC and strong absorption from the infiltrated and overlying perovskite material. This strategy, in which structural color and absorption are combined, is analogue to that found in beetles and may be considered, on these grounds, biomimetic.[24]

We performed an in-depth experimental and theoretical analysis of the optical effects occurring in perovskite solar cells that integrate PCs. We developed a theoretical model using a method based on the transfer matrix formalism, which allows us to calculate the electric field intensity within the layered structure and, thus, to visualize the effect of integrating the PC on the spatial distribution of the radiation in the photovoltaic device. Full details on the model can be found elsewhere, as well as evidence of its suitability to describe the optics of perovskite solar cells.[25] We fitted the experimental reflectance spectra of PC based cells measured at normal incidence, using the thickness of each layer in the structure extracted from the SEM as input parameters. Small variations around these reference values were permitted in the code in order to attain a fine-tuning of the calculated reflectance and hence a proper fitting. Good agreement between theory and experiment is attained, as displayed in Figure 2a. From the calculation, the unit cells of the periodic stacks are estimated to be 129 nm (d_H = 39 nm, d_L = 90 nm, for the TiO_2 and SiO_2 layers comprising the unit cell, respectively) for the PC based *blue-green* cell, and 145 nm (d_H = 58 nm, d_L = 87 nm) for the *orange* cell. Please note that the notation for the ranges herein employed to identify the color of the cells is the one commonly employed in CIE (*Comission Internationale de lÉclairage*) color diagrams. Such reflectance spectra can also be considered as the complementary of the absorptance spectra because light transmission through the cells is null. In that regard, each photonic design leads to a different field intensity distribution along the cell and hence to a different spatial and spectral distribution of optical absorption in the device. In Figure 2b–c, we show the way in which the optical field is distributed within the multilayer for the two cases chosen as examples. For comparing, we note the strong difference of light field distribution for photons with wavelength around 700 nm, whose penetration is much enhanced in the *blue-green* case, in comparison to the *orange* structure. This allows us to estimate the amount of light that is captured by each absorbing layer in the perovskite cell, which is provided as Supporting Information (Figure S3), and hence to discriminate between

DOI: 10.1021/nl504349z
Nano Lett. 2015, 15, 1698–1702

Table 1. Solar Cell Performance Parameters

device color		J_{sc} (mA/cm^2)	PCE (%)	V_{oc} (V)	FF
blue	best	13.4	8.8	0.98	0.67
	average	12.1 ± 1.2	7.6 ± 0.9	0.94 ± 0.02	0.67 ± 0.02
blue-green	best	10.4	7.0	0.95	0.71
	average	10.1 ± 0.3	6.5 ± 0.4	0.93 ± 0.02	0.68 ± 0.03
green	best	9.9	6.7	0.92	0.74
	average	9.4 ± 0.4	6.0 ± 0.4	0.92 ± 0.02	0.69 ± 0.03
orange	best	9.9	6.6	0.95	0.71
	average	8.9 ± 0.9	5.4 ± 0.8	0.91 ± 0.03	0.66 ± 0.05
red	best	7.6	4.5	0.93	0.62
	average	7.2 ± 0.5	4.1 ± 0.4	0.91 ± 0.02	0.61 ± 0.01

productive (absorbed in the perovskite material) and parasitic (absorbed in other components such as FTO) absorption.[25]

The device owes its color to the convolution of the reflectance spectrum that results from the interference of all beams partially transmitted and reflected at each interface in the device with the photopic response of the human eye. In order to characterize the color hue of the PC based photovoltaic device, we calculate their color coordinates and display the results as black symbols on the CIE 1931 chromaticity diagram in Figure 2d. By making use of our theoretical model, we have also extrapolated the full range of colors that can be eventually achieved by varying the thickness of the layers comprising the PCs infiltrated by perovskite. Such colors are encompassed by the dashed polygon in Figure 2d, which represents the PC-based cell tone gamut. Related to the appearance of the cells, structural colors are known to vary with the angle of observation, as they result from interference effects that are sensitive to the direction of illumination. However, in contrast to incorporating a chromatic filter in the surface of the outer glass, the integration of the PC within the solar cell strongly reduces the angular variability of the perceived color, as we described in Figure S4 of the Supporting Information. This could be advantageous where consistent coloration with angle is desired in a determined environment, such as buildings.

In Figure 3, we show the photovoltaic performance of perovskite solar cells displaying different colors. If the light is being reflected, it is not being absorbed, and hence, we expect there to be a trade-off between color and photocurrent generation for these solar cells. In Figure 3a–c, we show the different spectral response of the external quantum efficiency (EQE) measured from perovskite solar cells integrating orange and blue-green reflecting PCs as well as of a reference solar cell, made using a mesoporous SiO_2 scaffold with a thickness of ca. 370 nm. As expected, the EQE curves show clear depletions in those spectral regions for which the PC scaffold presents its reflectance maximum (shaded in gray in Figure 3b and c). Other potentially relevant effects such as photonic band gap edge absorption enhancement,[26] are not readily detectable in these measurements. In Figure 3d–g, we present the performance parameters for a series of solar cells made using photonic scaffolds that display a range of optical reflectance peaks. Measurements were taken under simulated AM1.5 sun light, at 100 mW cm^{-2} irradiance, with the parameters summarized in Table 1. The first encouraging observation is that the solar cells operate well, despite the requirement for conduction through the PC, consistent with the perovskite absorber bridging the conduction through the photonic scaffold. The short circuit current density (J_{sc}) monotonically decreases with the increase of the PC lattice parameter, as the color shifts from blue to red. However, the open-circuit voltage (V_{oc}) and fill factor (FF) are only slightly varying, displaying independence of the PC lattice parameter and indicating that the observed differences in photovoltaic performance have predominantly a photonic origin. We also observe that for blue, blue-green, green and orange hues, the power conversion efficiency (PCE) of the best performing devices are all above 6%, with the peak of 8.8% being achieved for the blue cells, showing good potential for making efficient working devices with vivid and tunable colors. As a comparison, we show the performance of the reference cell in Supporting Information Figure S5, which exhibits a peak and average PCE of 10.5 and 9.5%, respectively, indicating reasonable retention of the expected performance for the PC perovskite solar cells. We note that a current widely adopted technology for BIPV is amorphous silicon, where the BIPV modules integrated with a red-orange hue are less than 5% efficiency, illustrating potential for much superior performance for the colorful perovskite modules. Our work represents another example of the successful integration of multilayer structures with photonic properties in PV devices aiming at modifying their appearance without being detrimental for their performance.[21,27,28] In Figure 3h–j, we show photographs of the blue, green, and orange cells. The complete color palette is shown in the Supporting Information (see Figure S6). In addition, PC based solar cells show a good stabilized power output, which is the PCE measured under constant load and illumination.[29] As an example, a blue cell that showed a maximum JV determined efficiency of 7.9% and exhibited a stabilized power output of 6.6%. Results are also provided as Supporting Information (Figure S7).

In summary, we have demonstrated that a porous photonic crystal, built from alternating liquid processed layers of dense TiO_2 and porous SiO_2, can be constructed and integrated as a substitute scaffold into the active layer of a perovskite solar cell. The resulting solar cells exhibit well-defined reflectance bands, with the remaining nonreflected light being channelled into the perovskite absorber to undergo photovoltaic conversion at high efficiency. Aesthetically attractive perovskite solar cells in blue, blue-green, and green hues are now achievable and offer a new avenue for efficient and colorful PV for integration into the built environment. Key advantages of this route, as opposed to employing a colorful absorber layer, are that the structural color is unlikely to bleach or fade with time, and in addition, a single panchromatic photovoltaic absorber optimized for efficiency and stability can be integrated with a broad range of color hues. An unexpected advantage of the colorful perovskite solar cells for BIPV applications may be that the additional reflected light will reduce the thermal gain within the solar cell and in the

DOI: 10.1021/nl504349z
Nano Lett. 2015, 15, 1698–1702

building, which may have added benefits of lower operating temperatures of the solar cells, and hence increasing efficiency under real world conditions, reducing the cooling demand in buildings. We expect future improvements to be made by understanding and enhancing the electronic properties of the photonic crystal scaffolds, narrowing the reflectance bands and further optimization of the perovskite solar cells. This structure will also lend itself to perovskite light emitting diodes and may prove to be important for the realization of perovskite injection lasers. This method may also be applicable to a broader range of solution processed photovoltaic or light emitting materials.

■ ASSOCIATED CONTENT

Supporting Information

Method details, additional device performance, SEM image, absorptance and reflectance spectra, color hues analysis. This material is available free of charge via the Internet at http://pubs.acs.org.

■ AUTHOR INFORMATION

Corresponding Authors

*E-mail: h.miguez@csic.es.

*E-mail: h.snaith1@physics.ox.ac.uk.

Author Contributions

[§]These authors contributed equally to this work.

W.Z. and M.A. were in charge of the photonic crystal based perovskite solar cell design, preparation and characterization. Both of them contributed equally to this work. G.L. performed all the optical modeling of the cells and the color hue analysis. M.E.C. was in charge of optimizing the photonic crystal structure for integration in the solar cell and of SEM characterization. M.B.J. performed the EQE measurement. H.J.S. and H.M. supervised the work and wrote the manuscript.

Notes

The authors declare no competing financial interest.

■ ACKNOWLEDGMENTS

The research leading to these results has received funding from the EPSRC Supergen, the European Research Council under the European Union's Seventh Framework Programme (FP7/2007-2013)/ERC grant agreement no. 307081 (POLIGHT) and HYPER Project, the Spanish Ministry of Economy and Competitiveness under grant MAT2011-23593 and the Junta de Andalucía under grant FQM5247. M.A. is grateful to "La Caixa" Foundation for its financial support. FESEM characterization was performed at CITIUS, and we are grateful for its support. W.Z. thanks Ms Mingzhen Liu for providing vapor-deposited film sample.

■ ABBREVIATIONS

PV, photovoltaic; PCs, photonic crystals; BIPV, building integrated photovoltaics; spiro-OMeTAD, 2,2′,7,7′-tetrakis(*N*,*N*-di-*p*-methoxyphenylamine)-9,9′-spirobifluorene; FTO, fluorinated tin oxide; PCE, power conversion efficiency; J_{sc}, short-circuit current density; FF, fill factor; V_{oc}, open-circuit voltages; EQE, external quantum efficiency; SEM, scanning electron microscopy

■ REFERENCES

(1) Henemann, A. *Renewable Energy Focus* **2008**, *9*, 14−19.

(2) Kojima, A.; Teshima, K.; Shirai, Y.; Miyasaka, T. *J. Am. Chem. Soc.* **2009**, *131*, 6050−6051.

(3) Kim, H.-S.; Lee, C.-R.; Im, J.-H.; Lee, K.-B.; Moehl, T.; Marchioro, A.; Moon, S.-J.; Humphry-Baker, R.; Yum, J.-H.; Moser, J. E.; Grätzel, M.; Park, N.-G. *Sci. Rep.* **2012**, 2.

(4) Lee, M. M.; Teuscher, J.; Miyasaka, T.; Murakami, T. N.; Snaith, H. J. *Science* **2012**, *338*, 643−647.

(5) Burschka, J.; Pellet, N.; Moon, S.-J.; Humphry-Baker, R.; Gao, P.; Nazeeruddin, M. K.; Grätzel, M. *Nature* **2013**, *499*, 316−319.

(6) Liu, M.; Johnston, M. B.; Snaith, H. J. *Nature* **2013**, *501*, 395−398.

(7) Heo, J. H.; Im, S. H.; Noh, J. H.; Mandal, T. N.; Lim, C.-S.; Chang, J. A.; Lee, Y. H.; Kim, H.-j.; Sarkar, A.; Nazeeruddin, M. K.; Grätzel, M.; Seok, S. I. *Nat. Photonics* **2013**, *7*, 486−491.

(8) Liu, D.; Kelly, T. L. *Nat. Photonics* **2014**, *8*, 133−138.

(9) Zhou, H.; Chen, Q.; Li, G.; Luo, S.; Song, T.-b.; Duan, H.-S.; Hong, Z.; You, J.; Liu, Y.; Yang, Y. *Science* **2014**, *345*, 542−546.

(10) Jeon, N. J.; Noh, J. H.; Kim, Y. C.; Yang, W. S.; Ryu, S.; Seok, S. I. *Nat. Mater.* **2014**, *13*, 897−903.

(11) Im, J.-H.; Jang, I.-H.; Pellet, N.; Grätzel, M.; Park, N.-G. *Nat. Nanotechnol.* **2014**, *9*, 927−932.

(12) Green, M. A.; Ho-Baillie, A.; Snaith, H. J. *Nat. Photonics* **2014**, *8*, 506−514.

(13) Snaith, H. J. *J. Phys. Chem. Lett.* **2013**, *4*, 3623−3630.

(14) Noh, J. H.; Im, S. H.; Heo, J. H.; Mandal, T. N.; Seok, S. I. *Nano Lett.* **2013**, *13*, 1764−1769.

(15) Eperon, G. E.; Stranks, S. D.; Menelaou, C.; Johnston, M. B.; Herz, L. M.; Snaith, H. J. *Energy Environ. Sci.* **2014**, *7*, 982−988.

(16) Eperon, G. E.; Burlakov, V. M.; Goriely, A.; Snaith, H. J. *ACS Nano* **2014**, *8*, 591−598.

(17) Roldan-Carmona, C.; Malinkiewicz, O.; Betancur, R.; Longo, G.; Momblona, C.; Jaramillo, F.; Camacho, L.; Bolink, H. J. *Energy Environ. Sci.* **2014**, *7*, 2968−2973.

(18) Ono, L. K.; Wang, S.; Kato, Y.; Raga, S. R.; Qi, Y. *Energy Environ. Sci.* **2014**, *7*, 3989−3993.

(19) Colodrero, S.; Mihi, A.; Häggman, L.; Ocana, M.; Boschloo, G.; Hagfeldt, A.; Miguez, H. *Adv. Mater.* **2009**, *21*, 764−770.

(20) Betancur, R.; Romero-Gomez, P.; Martinez-Otero, A.; Elias, X.; Maymo, M.; Martorell, J. *Nat. Photonics* **2013**, *7*, 995−1000.

(21) Ball, J. M.; Lee, M. M.; Hey, A.; Snaith, H. J. *Energy Environ. Sci.* **2013**, *6*, 1739−1743.

(22) Colodrero, S.; Ocaña, M.; Míguez, H. *Langmuir* **2008**, *24*, 4430−4434.

(23) Brinker, C. J.; Frye, G. C.; Hurd, A. J.; Ward, K. J.; Ashley, C. S. *J. Non-Cryst. Solids* **1990**, *121*, 294−302.

(24) Kolle, M. *Photonic structures inspired by nature*. Springer: New York, 2011.

(25) Anaya, M.; Lozano, G.; Calvo, M. E.; Zhang, W.; Johnston, M. B.; Snaith, H. J.; Miguez, H. *J. Phys. Chem. Lett.* **2015**, *6*, 48−53.

(26) Anaya, M.; Calvo, M. E.; Luque-Raigón, J. M.; Míguez, H. *J. Am. Chem. Soc.* **2013**, *135*, 7803−7806.

(27) Colonna, D.; Colodrero, S.; Lindström, H.; Di Carlo, A.; Miguez, H. *Energy Environ. Sci.* **2012**, *5*, 8238−8243.

(28) Lee, K.-T.; Lee, J. Y.; Seo, S.; Guo, L. J. *Light: Sci. Appl.* **2014**, *3*, e215.

(29) Snaith, H. J.; Abate, A.; Ball, J. M.; Eperon, G. E.; Leijtens, T.; Noel, N. K.; Stranks, S. D.; Wang, J. T.-W.; Wojciechowski, K.; Zhang, W. *J. Phys. Chem. Lett.* **2014**, *5*, 1511−1515.

DOI: 10.1021/nl504349z
Nano Lett. 2015, 15, 1698−1702